HHS Public Access

Author manuscript

Angew Chem Int Ed Engl. Author manuscript; available in PMC 2023 September 12.

Published in final edited form as:

Angew Chem Int Ed Engl. 2022 September 12; 61(37): e202209227. doi:10.1002/anie.202209227.

Thiol-Disulfide Exchange as a Route for Endosomal Escape of Polymeric Nanoparticles

Pintu Kanjilal,
Department of Chemistry, University of Massachusetts Amherst, Amherst, MA 01003, United States

Kingshuk Dutta,
Department of Chemistry, University of Massachusetts Amherst, Amherst, MA 01003, United States

S Thayumanavan[*]
Department of Chemistry, Department of Biomedical Engineering, Molecular and Cellular Biology Program, and Centre for Bioactive Delivery-Institute for Applied Life Sciences, University of Massachusetts Amherst, Amherst, MA 01003, United States

Abstract

Endosomal entrapment has remained the major bottleneck for cytosolic delivery of nanoparticle-based delivery systems. Uncovering fundamentally new pathways for endosomal escape is therefore highly sought. Herein, we report that disulfide bonds can enhance endosomal escape through contacts with cellular exofacial thiols, in addition to facilitating cellular uptake. Our results are supported through comparative analysis of polymeric nanogels with variable accessibility to disulfide bonds by placing these functionalities at the core or the shell of the nanogels. The findings here inform future chemical design of delivery vehicles.

Graphical Abstract

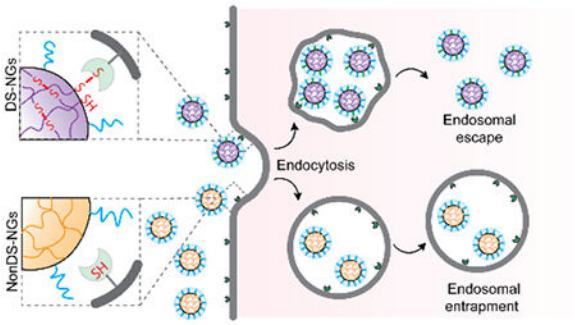

Polymeric nanogels with judiciously placed disulfide bonds have been synthesized and tested for cellular uptake and endosomal escape. Comparison with their non-disulfide counterparts show that disulfide moieties play a key role in endosomal escape.

[*] thai@umass.edu .

Keywords

Polymeric nanogel; Disulfide bond; Endosomal entrapment; Endosomal Escape

Polymer-based nanoparticles have been used extensively for therapeutics delivery to mitigate poor stability and cellular uptake of bioactive molecules.[1–4] The most dominant route of cellular entry for nanoparticles is through endocytosis, where these drug carriers are initially trapped in vesicular endosomes.[5–6] Considering that the therapeutic activity of these molecules occur in the cytosol or other sub-cellular compartments besides the lysosome, escape of the nanocarriers from the endosome is critical for success for therapies involving intracellular targets. In fact, endosomal escape is generally recognized as the major bottleneck for nanoparticle-based delivery systems.[7–10] Strategies to induce endosomal escape often leverage intrinsic stimuli that cause induced membrane disruption of the endosome.[11] Examples include incorporation of functionalities that enhance pH buffering in endosomes, fusion with endosomal membranes, incorporation of endosomolytic agents in the carrier, and utilization of cell penetrating peptides.[12–18] So far however, robust design guidelines that offer reliable endosomal escape of nanocarriers have not been developed. Thus, there is a dire need for new strategies that improve endosomal escape.

Disulfide-containing molecules and polymers have been recently shown to exhibit enhanced cellular uptake and cytosolic localization, which is attributed to a non-classical pathway involving cell surface thiols.[19–20] For example, cell penetrating poly(disulfide)s have been developed to achieve direct cellular internalizations of molecules that bypass endocytosis.[21–25] While it is plausible for single molecules to be taken up through this non-classical pathway, we surmised that it is unlikely that larger cargo-bearing nanoparticles would go through any uptake pathway other than the endosomal one. To our knowledge, the effect of disulfide bonds in the cellular uptake or endosomal escape has not been investigated in nanoparticles. This is surprising, considering the fact that disulfide-based nanoparticles have been of great general interest in deliver applications, because of their redox responsiveness to intracellular glutathione.[26–29] In the work here, we study the impact of disulfide functionalities on both cellular entry and endosomal escape of nanoparticles. Although nanoparticles do enter cells through the endosome, we find here that disulfide functionalities specifically endow them with the ability for endosomal escape (Figure 1).

We hypothesized that a potential covalent contact between disulfide-bearing nanoparticles and exofacial thiols would not only facilitate cellular uptake, but also enhance endosomal escape of these nanoparticles. The premise for this idea involves the possibility that the randomized multiple covalent contacts between the thiols of cellular/endosomal membrane[30] will necessarily deform the membrane. We envisioned that such a strain on the membrane would facilitate endosomal escape, as schematically illustrated in Figure 1. To test this hypothesis, we designed polymeric nanogels with and without disulfide-based crosslinkers as candidate nanoparticles. Disulfide-containing nanogels (DS-NGs) were synthesized using the self-crosslinking of pyridyl disulfide-based side chains (Scheme 1).[31–34] Similar nanogels without disulfide bonds (NonDS-NGs) were accessed by crosslinking pentafluorophenylester based polymers with tetraethyleneglycol diamine

(Scheme 1).[35] Details on the syntheses and characterizations of these nanogels are described in the Supporting Information. Relative efficiency of cellular uptake was first assessed for the DS-NGs and NonDS-NGs. Similar to that observed with small molecules and polymers,[22–23] we anticipated that the disulfide bonds in DS-NGs might facilitate cellular uptake. To test this, both nanogels were functionalized with the Sulfo-Cy3 dye (Figure S1, S2) to facilitate fluorescent monitoring of cellular uptake. Flow cytometry was used to compare cellular internalizations. Despite their similarity in size and zeta potential (DS-NGs: 10 nm and −27 mV; NonDS-NGs: 10 nm and −33.8 mV) (Figure: S6, S7 & S8), we observed a ~4-fold increase in uptake in EMT6 cells for DS-NG, compared to NonDS-NG (Figure 2a). We surmised that the higher uptake of DS-NGs could be attributed to the interaction between disulfides in the nanogel and cell surface thiols. To test this, we masked the cell surface thiols with Ellman's reagent (DTNB) and sodium iodoacetate, which reduce the thiol-disulfide exchange reaction on cell surface.[21] Following these treatments, we observed a ~20% and ~50% reduction in cell uptake of DS-NGs respectively, while no such change in uptake was observed with NonDS-NGs (Figure 2b). To ensure that any of the observed differences are not due to cytotoxicity of the nanogels, we evaluated both nanogels for toxicity with an alamarBlue assay and found both nanogels to be non-toxic to cells (Figure S9). To assess if DS-NG does indeed have accessible disulfide moieties, we quantified the surface exposed disulfides on nanogels by reacting with a thiol-functionalized water-soluble fluorophore (Z-Rhodamine-SH). Based on the UV-vis spectra, we found that the concentration of surface exposed disulfides to be ~0.51 μM in 1 mg/mL concentration of the nanogel (Figure 2c and S10).

Although small molecules and polymer chains have been shown to be taken up through a non-classical cellular entry, we suspected that these nanogels (and most nanoparticles) would enter the cells through an endosomal pathway. To assess this, we studied the uptake of DS-NGs and NonDS-NGs nanogels in the presence inhibitors comprising all uptake pathways.[36] As shown in Figure 2d, the sucrose and NaN_3/2-deoxy-D-glucose treatments caused significant inhibition in cellular uptake of DS-NGs, suggesting clathrin-mediated pathway to be the predominant mode of internalization. This observation is consistent with a literature report, where a disulfide containing-amino acid tagged proapoptotic protein was endocytosed predominantly via clathrin-mediated endocytosis.[37] The non-significant uptake of DS-NGs at 4 °C further confirms the dominant internalization mode to be endocytosis over direct uptake. On the other hand, NonDS-NGs internalizations was affected by EIPA, cytochalasin D, dyngo and sucrose, indicate a combination of uptake pathways (Figure S11). To further understand the internalization process, we conjugated DS-NGs with a different fluorophore (AF488) and studied the simultaneous intracellular trafficking with sulfo-cy3 tagged NonDS-NGs nanogel. As Figure S13 shows, a predominant colocalized yellow fluorescence at 4 h indicates a commonality in internalization routes for both nanogels. Once the uptake pathway is established as endosomal, we evaluated the relative propensity of the two nanogels to escape the endosome. Following cellular uptake, we monitored the colocalization of fluorescently-labeled nanogels with LysoTracker Green™ using confocal microscopy to assess endosomal escape. As shown in Figure 3a, DS-NGs exhibit significant endosomal escape, as evident by the independent fluorescent color from LysoTracker Green and the Cy3-labeled nanogel. Even a few sparse yellow fluorescence spots, indicating

endosomal entrapment, were resolved at the 42 h time period. On the contrary, the NonDS-NGs were completely colocalized with LysoTracker Green not only at 18 h, but persisted even after 42 h, indicating endosomal entrapment (Figure 3b).

To further quantify the extent of colocalizations, we calculated the Pearson's coefficient for both nanogels (Figure 3c, e). A high Pearson's coefficient number indicates co-localization of fluorescence, which makes the datapoints in the plot to fall along the diagonal.[36] Divergence of the points from the diagonal indicate disparate location of the two fluorescences, which is indicated with a lower Pearson's coefficient. For the NonDS-NGs, a Pearson's value of 0.82 at 42 h was observed, whereas a bifurcated distribution of fluorescence for the DS-NGs resulted in the Pearson's value of 0.38. We also analyzed the temporal evolution of endosomal escape by testing the time-dependent changes in the Pearson's coefficient for both nanogels. We did not observe any change in the Pearson's coefficient for NonDS-NGs nanogel over the entire 42 h time period (Figure 3d, S14), whereas the coefficient continuously decreased from an already lower 0.60 at 1 h to 0.38 at 42 h (Figure 3f, S15). Despite the clearly low Pearson's coefficient, the DS-NGs also exhibit punctate cytosolic fluorescence, which is often attributed to endosomal entrapment.[7–8,11] We attribute this observation to the possible aggregation of the amphiphilic polymer and nanogels in the cytosol. As the Cy3 fluorophore is chemically conjugated to the nanogel, the aggregate formation would translate to localized, punctate fluorescence. To test this possibility, we non-covalently encapsulated Nile red into the DS-NGs, instead of covalently attaching a dye molecule. In this case, as the DS-NGs are uncrosslinked due to the cytosolic glutathione, the non-covalently encapsulated Nile red should be liberated, and the fluorescence should not be punctated. Indeed, the cytosolic fluorescence from Nile red was quite diffused in the cytosol (Figure S16).

To further confirm that the NonDS-NGs lacked endosomal escape properties, we used chloroquine diphosphate (CQ) to induce endosomal osmotic pressure and release the nanogels in the cytosol.[32–33] Indeed, upon cotreatment of the cells with NonDS-NGs and CQ, significant endosomal escape is observed, while CQ did not have a significant effect on the endosomal escape outcome with the DS-NGs (Figure S17). Additionally, we have also monitored the separation of colocalized fluorescence of AF488 conjugated DS-NGs and sulfo-cy3 labeled NonDS-NGs nanogels at longer time scale. As Figure S18 shows, we observed appearance of independent fluorescence at 42 h which supports the release both particles from endosome. Overall, these results clearly suggest that DS-NGs exhibit a much better tendency to not only enter the cells, but also to escape the endosome.

If the disulfide-based interaction between the cell surface thiols and nanogel disulfides hold the key for the observed cellular uptake and endosomal escape, then increased exposure of the disulfide functionalities to the outer surface of the nanogels should even further enhance their cellular uptake and endosomal escape. To test this idea, we developed structurally similar nanogels with disulfides exposed in their periphery, PeriDS-NGs (Figure 4a). To this end, we synthesized a polymer that is primarily based on a polyethyleneglycol (PEG) methacrylate that is terminated with a pyridyl disulfide functionality. The inherent amphiphilicity of the side chain functionalities was used to form nanoaggregates which are in situ crosslinked to achieve the PeriDS-NGs. The surface exposed disulfide on PeriDS-

NGs nanogel was quantified to be 0.76 μM in 1 mg/mL concentration of the nanogel, when assessed by reacting with the thiol-functionalized Z-Rhodamine-SH (Figure S24a). We compared the internalization of PeriDS-NGs with DS-NGs using flow cytometry and confocal microscopy. We were gratified to observe that a significant increase in cellular uptake of PeriDS-NGs (Figure S24b). As Peri-DS-NGs were found to be about ~100 nm, we also considered that their higher internalization could arise from its bigger size (the DS-NGs above were ~10 nm in size). To verify that, we synthesized of DS-NGs to a comparable size to PeriDS-NGs and compared the nanogel internalization (Figure S25a). We did find that 100 nm DS-NG nanogel exhibits ~3-fold higher cellular uptake, compared to 10 nm nanogel. However, that the PeriDS-NGs internalization is still substantially higher than that of the 100 nm DS-NGs, which supports the role of exposed disulfides on the nanogel surface. We further tested the effect of exposed disulfide functionalities, cell surface thiols of PeriDS-NGs were blocked by DTNB and iodoacetate, which was found to reduce uptake of by ~30% and ~60% respectively (Figure S27b). Higher reduction in cellular uptake, compared to DS-NGs, further supports the role of the disulfide bonds in interaction with cell surface thiols.

We then evaluated the propensity of Peri-DS-NGs to escape the endosome with lysotracker colocalization studies, where we found that these nanogels exhibit efficient endosomal escape even at 18 h (Figure S28a). The Pearson's coefficient for Peri-DS-NGs was found to be 0.39 at 18 h, which further decreased to 0.31 at 42 h, supporting more efficient endosomal escape compared to both NonDS-NGs and DS-NGs. The temporal evolution of Pearson's coefficient further supported the efficient endosomal escape of PeriDS-NGs nanogels (Figure S28c). Overall, disulfides were found to be crucial in enhancing the cellular uptake of the nanogels and their endosomal escape.

We were further interested in using a complementary assay to evaluate the endosomal escape. We used calcein as a probe for this purpose, which is a membrane-impermeable fluorophore that enters the cells through the endosome. In endosomes, calcein exhibits punctate and lower fluorescence at high self-quenching concentrations. When liberated from the endosome, calcein is present throughout the cytosol and exhibits high fluorescence due to reduced self-quenching. Thus, upon coincubation with endosomolytic particles, calcein releases from the endosome and exhibits strong and diffused fluorescence throughout the cytosol (Figure S19).[38–41] When EMT6 cells are treated with PeriDS-NGs and DS-NGs, along with calcein, diffused fluorescence is observed throughout the cytosol indicating efficient endosomal escape. On the other hand, both untreated control (*i.e.,* only calcein) and those treated with NonDS-NGs cell remain punctate fluorescence, indicating endosomal entrapment (Figure 4c). A time dependent cotreatment of calcein with DS-NGs (Figure S20) and PeriDS-NGs (Figure S29) showed the gradual diffused fluorescence over time confirms the endosomal escape of disulfide particles. We also observed a few diffused cells at 1 h itself which indicates that a smaller fraction of the of nanogels can be internalized via other pathways which can result in the lower Pearson's coefficient at initial hour.

In summary, we have demonstrated the effect of disulfide bonds in polymeric nanogels towards endosomal escape. Three different polymeric nanogels have been synthesized with strategically different positioning of disulfide bonds. Cellular uptake and endosomal

escape capabilities of these nanogels are then assessed, which show that disulfide-containing nanogels (DS-NGs) could escape the endosome, whereas non-disulfide nanogels (NonDS-NGs) remain entrapped. Exposing the disulfides on the outer surface of the nanogel further enhances both cellular uptake and endosomal escape. Temporal evolution of the endosomal escape supports the assertion that disulfide bonds play a critical role in the observed endosomal escape. The mechanism that underlies the observed endosomal escape is not clear at this time. We provisionally propose that the covalent contact between the membrane thiols and the nanogel strains the packing of the endosomal membranes (Figure 1). The propensity to relieve this strain is presumably the driving force for endosomal escape. As endosomal escape is a major bottleneck in delivering small molecule therapeutics and biologics inside the cells, identification of this new pathway for endosomal escape will open up new design strategies for therapeutic delivery.

Supplementary Material

Refer to Web version on PubMed Central for supplementary material.

Acknowledgements

We thank NIGMS of the NIH for support (GM-136395). We thank Drs. Khushboo Singh and Ziwen Jiang for helpful discussions. We also thank Dr. James Chambers and Dr. Amy Burnside in UMass Light Microscopy Center and Flow Cytometry Facility respectively for experimental suggestions.

References

[1]. Shi J, Kantoff PW, Wooster R, Farokhzad OC, Nat. Rev. Cancer 2017, 17, 20–37. [PubMed: 27834398]

[2]. Qin X, Yu C, Wei J, Li L, Zhang C, Wu Q, Liu J, Yao SQ, Huang W, Adv. Mater 2019, 31, 1902791.

[3]. Revia RA, Stephen ZR, Zhang M, Acc. Chem. Res 2019, 52, 1496–1506. [PubMed: 31135134]

[4]. Li Y, Li P, Li R, Xu Q, Adv. Therap 2020, 3, 2000178.

[5]. Martens TF, Remaut K, Demeester J, De Smedt SC, Braeckmans K, Nano Today 2014, 9, 344–364.

[6]. Behzadi S, Serpooshan V, Tao W, Hamaly MA, Alkawareek MY, Dreaden EC, Brown D, Alkilany AM, Farokhzad OC, Mahmoudi M, Chem. Soc. Rev 2017, 46, 4218–4244. [PubMed: 28585944]

[7]. Smith SA, Selby LI, Johnston AP, Such GK, Bioconjugate Chem 2019, 30, 263–272.

[8]. Pei D, Buyanova M, Bioconjugate Chem 2018, 30, 273–283.

[9]. Spicer CD, Jumeaux C, Gupta B, Stevens MM, Chem. Soc. Rev 2018, 47, 3574–3620. [PubMed: 29479622]

[10]. Chou LY, Ming K, Chan WC, Chem. Soc. Rev 2011, 40, 233–245. [PubMed: 20886124]

[11]. Selby LI, Cortez-Jugo CM, Such GK, Johnston AP, WIREs Nanomed. Nanobiotechnol 2017, 9, e1452.

[12]. Lin C, Engbersen JF, Control J. Release 2008, 132, 267–272.

[13]. Bus T, Traeger A, Schubert US, J. Mater. Chem. B 2018, 6, 6904–6918. [PubMed: 32254575]

[14]. Pack DW, Hoffman AS, Pun S, Stayton PS, Nat. Rev. Drug Discov 2005, 4, 581–593. [PubMed: 16052241]

[15]. Vermeulen LM, Brans T, Samal SK, Dubruel P, Demeester J, De Smedt SC, Remaut K, Braeckmans K, ACS Nano 2018, 12, 2332–2345. [PubMed: 29505236]

[16]. Goswami R, Jeon T, Nagaraj H, Zhai S, Rotello VM, Trends Pharmacol. Sci 2020, 41, 743–754. [PubMed: 32891429]

[17]. Nam HY, Kim J, Kim S, Yockman JW, Kim SW, Bull DA, Biomaterials 2011, 32, 5213–5222. [PubMed: 21501867]

[18]. Akishiba M, Takeuchi T, Kawaguchi Y, Sakamoto K, Yu HH, Nakase I, Takatani-Nakase T, Madani F, Gräslund A, Futaki S, Nat. Chem 2017, 9, 751–761. [PubMed: 28754944]

[19]. Laurent Q, Martinent R, Lim B, Pham AT, Kato T, López-Andarias J, Sakai N, Matile S, JACS Au 2021, 1, 710–728. [PubMed: 34467328]

[20]. Dutta K, Das R, Medeiros J, Thayumanavan S, Biochem 2021, 60, 966–990. [PubMed: 33428850]

[21]. Gasparini G, Sargsyan G, Bang EK, Sakai N, Matile S, Angew. Chem. Int. Ed 2015, 127, 7436–7439.

[22]. Gasparini G, Bang EK, Molinard G, Tulumello DV, Ward S, Kelley SO, Roux A, Sakai N, Matile S, J. Am. Chem. Soc 2014, 136, 6069–6074. [PubMed: 24735462]

[23]. Bej R, Ghosh A, Sarkar J, Das BB, Ghosh S, ChemBioChem 2020, 21, 2921–2926. [PubMed: 32424847]

[24]. Fu J, Yu C, Li L, Yao SQ, J. Am. Chem. Soc 2015, 137, 12153–12160. [PubMed: 26340272]

[25]. Yang W, Yu C, Wu C, Yao SQ, Wu S, Polym. Chem 2017, 8, 4043–4051.

[26]. Jiang Z, Cui W, Prasad P, Touve MA, Gianneschi NC, Mager J, Thayumanavan S, Biomacromolecules 2019, 20, 435–442. [PubMed: 30525500]

[27]. Dutta K, Kanjilal P, Das R, Thayumanavan S. Angew. Chem. Int. Ed 2021, 60, 1821–1830.

[28]. Oupický D, Li J, Macromol. Biosci 2014, 14, 908–922. [PubMed: 24678057]

[29]. Peng YY, Diaz-Dussan D, Kumar P, Narain R, Bioconjugate Chem 2019, 30, 405–412.

[30]. Stephan MT, J Moon J, Um SH, Bershteyn A, Irvine DJ, Nat. Med 2010, 16, 1035–1041. [PubMed: 20711198]

[31]. Ghosh S, Basu S, Thayumanavan S, Macromolecules 2006, 39, 5595–5597.

[32]. Ryu JH, Chacko RT, Jiwpanich S, Bickerton S, Babu RP, Thayumanavan S, J. Am. Chem. Soc 2010, 132, 17227–17235. [PubMed: 21077674]

[33]. Anson F, Liu B, Kanjilal P, Wu P, Hardy JA, Thayumanavan S, Biomacromolecules 2021, 22, 1261–1272. [PubMed: 33591168]

[34]. Anson F, Kanjilal P, Thayumanavan S, Hardy JA, Protein Sci 2021, 30, 366–380. [PubMed: 33165988]

[35]. Zhuang J, Jiwpanich S, Deepak VD, Thayumanavan S, ACS Macro Lett 2012, 1, 175–179.

[36]. Rennick JJ, Johnston APR, Parton RG, Nat. Nanotechnol 2021, 16, 266–276. [PubMed: 33712737]

[37]. Abegg D, Gasparini G, Hoch DG, Shuster A, Bartolami E, Matile S, Adibekian A, J. Am. Chem. Soc 2017, 139, 231–238. [PubMed: 28001050]

[38]. Beztsinna N, de Matos MBC, Walther J, Heyder C, Hildebrandt E, Leneweit G, Mastrobattista E, Kok RJ, Sci. Rep 2018, 8, 2768. [PubMed: 29426932]

[39]. Ren K, Liu Y, Wu J, Zhang Y, Zhu J, Yang M, Ju H, Nat. Commun 2016, 7, 13580. [PubMed: 27882923]

[40]. Dutta K, Bochicchio D, Ribbe AE, Alfandari D, Mager J, Pavan GM, Thayumanavan S, ACS Appl. Mater. Inter 2019, 11, 24971–24983.

[41]. Hong S, Leroueil PR, Janus EK, Peters JL, Kober MM, Islam MT, Orr BG, Baker JR, Banaszak Holl MK, Bioconjugate Chem 2006, 17, 728–734.

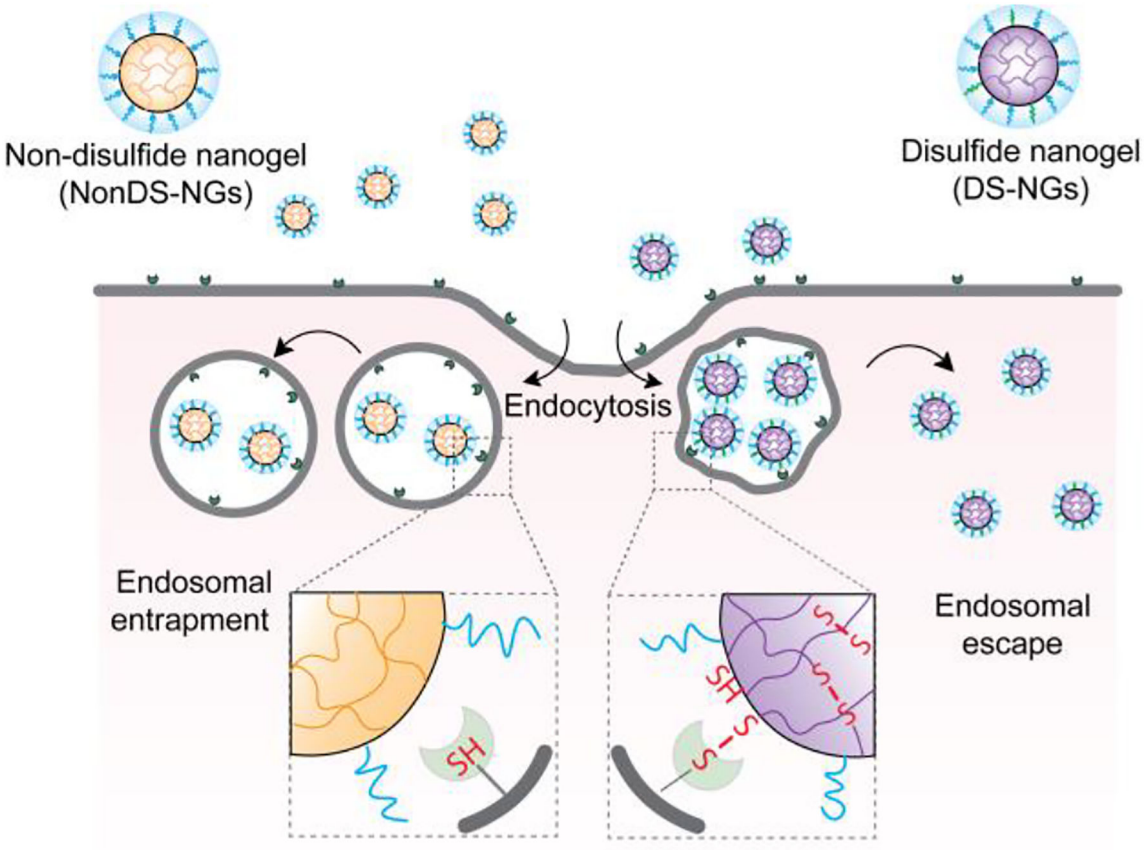

Figure 1:
Schematic representation of the proposed hypothesis on the role of disulfide bonds in endosomal escape of polymeric nanogels.

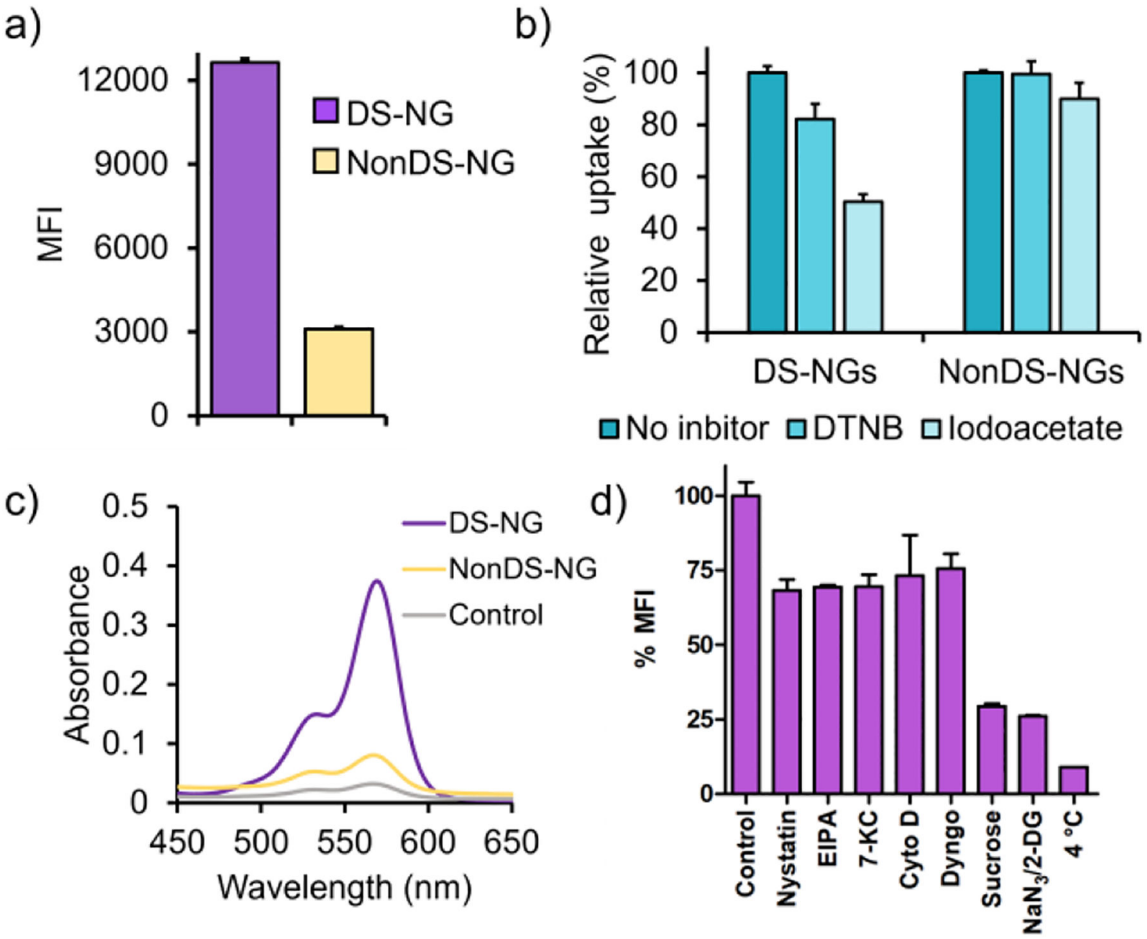

Figure 2:

Quantification of intracellular uptake and understanding the internalization pathways of nanogels. (a) Quantification of cellular uptake of nanogels; (b) Effect of DTNB and iodoacetate treatment on internalizations; (c) Quantification of surface exposed disulfide on nanogel ; (d) Mechanisms of cellular uptake of DS-NGs nanogels in presence and absence of inhibitors.

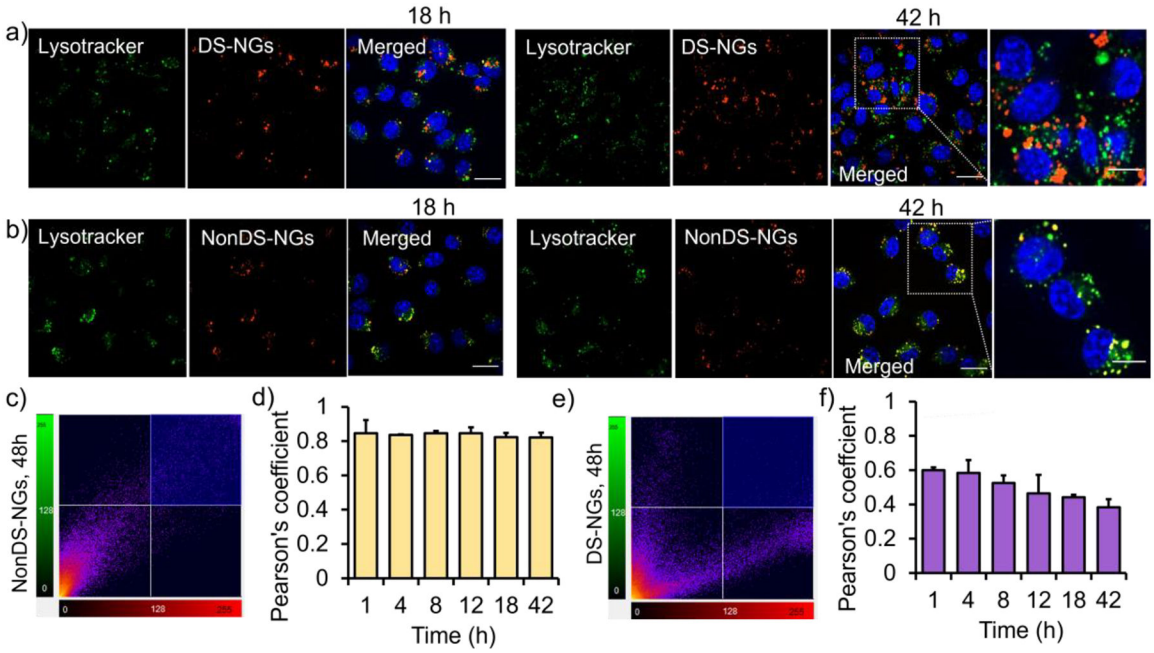

Figure 3:

Evaluation of endosomal escape in EMT6 cell line. (a) Confocal microscopy images showing the intracellular uptake of sulfo-cy3 labelled DS-NGs at 18 h and 42 h; (b) Intracellular uptake of sulfo-cy3 labelled NonDS-NGs particle at 18 h and 42 h, Scale bar 20 μm; (c) Pearson's correlation plot at 42 h and (d) temporal evaluation of Pearson's coefficient for NonDS-NGs; (e) and core disulfide particles at 42 h. (d) Pearson's correlation plot for DS-NGs at 42 h and the time dependent Pearson's coefficient evaluation

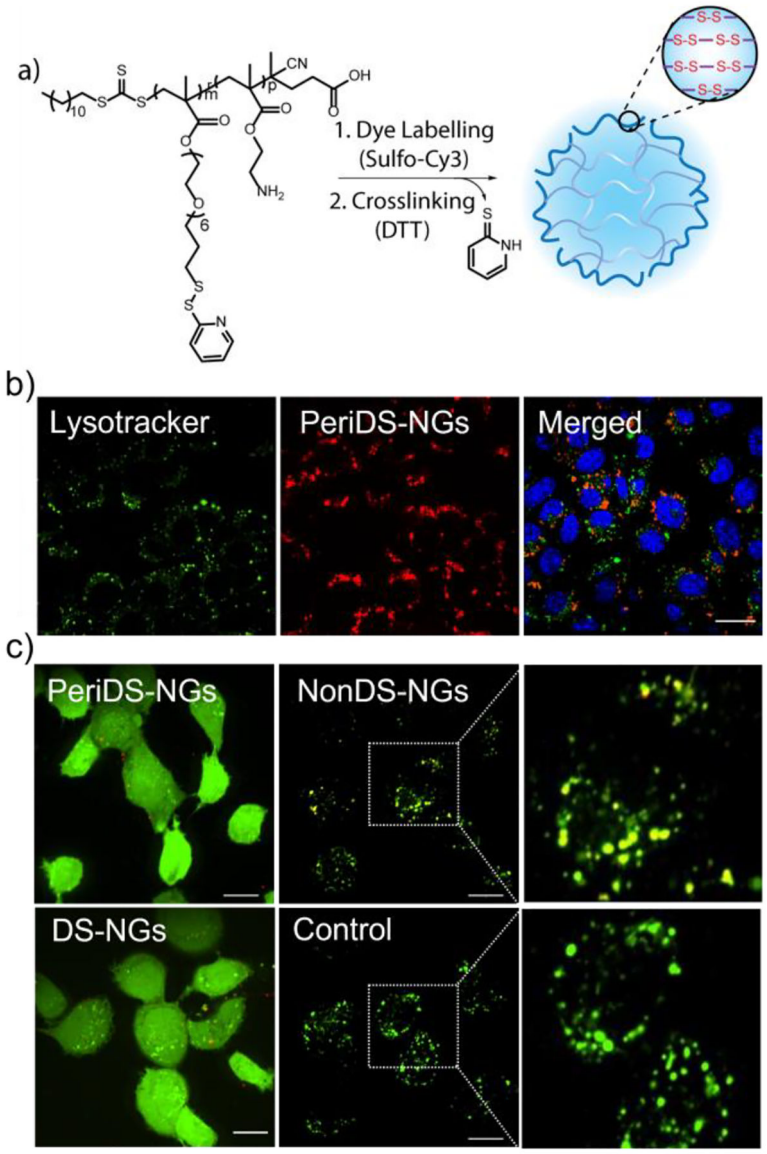

Figure 4:

(a) Reaction scheme for the synthesis of PeriDS-NGs nanogel; (b) Confocal microscopy image showing the endosomal escape profile at 48 h; (c) Calcein assay to evaluate the endosomolytic behavior of disulfide bonds in nanogels. PeriDS-NGs and DS-NGs showed diffused fluorescence, indicate the endosomal escape of disulfide containing nanogels. Whereas NonDS-NGs remained punctate with yellow colocalized fluorescence shows endosomal entrapment. Scale bar 20 μm.

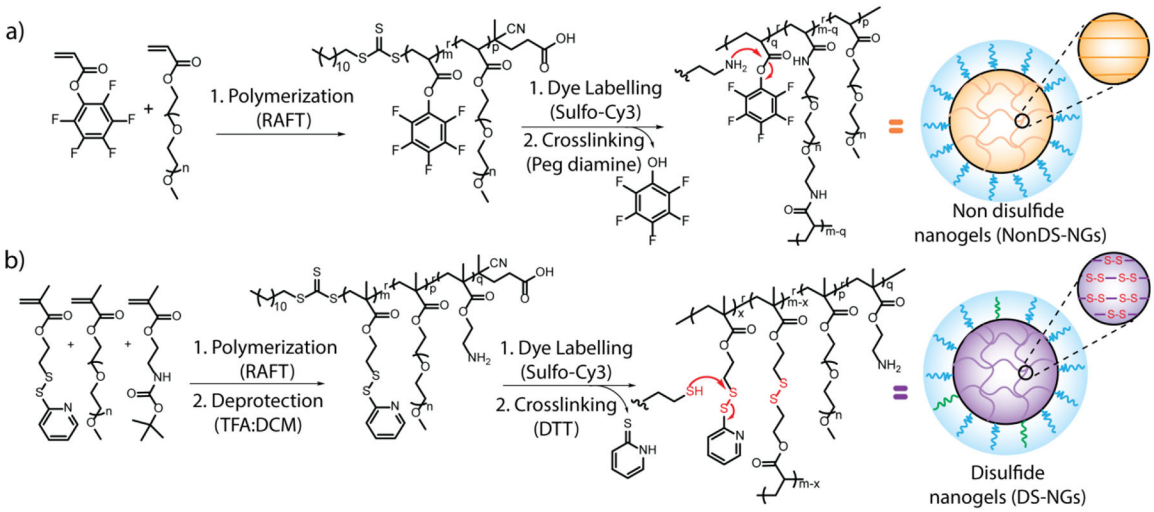

Scheme 1:

(a) Synthetic reaction schemes for $P_{NonDS\text{-}NGs}$ polymer and formation of NonDS-NGs. The relative percentages of monomers are m:p = 70:30; (b) Synthetic reaction scheme for $P_{DS\text{-}NGs}$ polymer followed by DS-NGs nanogel formation. The relative percenatages of m:p:q = 63:32:05.